
Since January 2020 Elsevier has created a COVID-19 resource centre with free information in English and Mandarin on the novel coronavirus COVID-19. The COVID-19 resource centre is hosted on Elsevier Connect, the company's public news and information website.

Virology 484 (2015) 170–180

Contents lists available at ScienceDirect

Virology

journal homepage: www.elsevier.com/locate/yviro

# Lipid rafts both in cellular membrane and viral envelope are critical for PRRSV efficient infection

Qian Yang [a,b], Qiong Zhang [a,b], Jun Tang [a,c], Wen-hai Feng [a,b,*]

[a] State Key Laboratory of Agrobiotechnology, China Agricultural University, Beijing 100193, China
[b] Department of Microbiology and Immunology, College of Biological Sciences, China Agricultural University, Beijing 100193, China
[c] Department of Basic Veterinary Medicine, College of Veterinary Medicine, China Agricultural University, Beijing 100193, China

ARTICLE INFO

*Article history:*
Received 29 December 2014
Returned to author for revisions
28 May 2015
Accepted 4 June 2015
Available online 23 June 2015

*Keywords:*
PRRSV
Lipid raft
CD163

ABSTRACT

Porcine reproductive and respiratory syndrome virus (PRRSV) represents a significantly economical challenge to the swine industry worldwide. In this study, we investigated the importance of cellular and viral lipid rafts in PRRSV infection. First, we demonstrated that PRRSV glycoproteins, Gp3 and Gp4, were associated with lipid rafts during viral entry, and disruption of cellular lipid rafts inhibited PRRSV entry. We also showed the raft-location of CD163, which might contribute to the glycoproteins–raft association. Subsequently, raft disruption caused a significant reduction of viral RNA production. Moreover, Nsp9 was shown to be distributed in rafts, suggesting that rafts probably serve as a platform for PRRSV replication. Finally, we confirmed that disassembly of rafts on the virus envelope may affect the integrity of PRRSV particles and cause the leakage of viral proteins, which impaired PRRSV infectivity. These findings might provide insights on our understanding of the mechanism of PRRSV infection.



## Introduction

Porcine reproductive and respiratory syndrome virus (PRRSV) is an enveloped, single-strand positive-sense RNA virus belonging to the family *Arteriviridae*, order *Nidovirales* (Collins et al., 1992; Conzelmann et al., 1993; Wensvoort et al., 1991). Its genome is approximately 15.4-kb containing a 5′- and a 3′-untranslated region (UTR) and 10 open reading frames (Conzelmann et al., 1993; Johnson et al., 2011; Meng et al., 1994; Meulenberg et al., 1993). It encodes at least 16 non-structural proteins involved in the processing of viral proteolysis, genome replication, transcription and evading host immune responses, which include four proteases (Nsp1α, Nsp1β, Nsp2, and Nsp4), the RNA-dependent RNA polymerase (Nsp9), a helicase (Nsp10), and an endonuclease (Nsp11) (Dokland, 2010; Fang et al., 2012; Snijder and Meulenberg, 1998; Ziebuhr et al., 2000). It also encodes eight structural proteins including the membrane glycoproteins Gp2a, Gp2b, Gp3, Gp4, Gp5, and Gp5a, the matrix protein (M), and the nucleocapsid protein (N) involved in the process of viral entry, assembling, and release (Dea et al., 2000; Johnson et al., 2011; Meulenberg et al., 1995). These viral proteins are associated with certain host factors to control the whole process of PRRSV infection.

PRRSV has two major genotypes, the European genotype (type 1) and the North American genotype (type 2) (Forsberg, 2005; Hanada et al., 2005). Recently, there have been devastating outbreaks of atypical PRRS caused by a highly pathogenic PRRSV (HP-PRRSV) strain in China, which is characterized by high fever, high morbidity, and high mortality in all age pigs (Zhou and Yang, 2010). PRRSV has a very narrow cell tropism, showing a preference for cells of the monocyte/macrophage lineage *in vivo* (Duan et al., 1997). PRSSV is also sustained by MA-104 cell line derived from African green monkey kidney and its derivatives (MARC-145 and CL2621) *in vitro* (Kim et al., 1993). This cell tropism is mainly determined by the presence or absence of specific receptors in the target cells. PRRSV enters cells via receptor-mediated endocytosis, and heparan sulfate, sialoadhesin, and CD163 are known as the main PRRSV receptors (Van Breedam et al., 2010a). CD163, a macrophage differentiation membrane antigen belonging to the scavenger receptor cysteine-rich (SRCR) family, is shown to be capable of mediating PRRSV infection in non-permissive cells (Calvert et al., 2007).

The plasma membrane is proposed not to be a homogeneously passive solvent, but a heterogeneous structure, displaying a tremendous complexity of lipids and proteins (Lingwood and Simons, 2010). The strong evidence for this theory is the presence of lipid rafts that are specialized lipid domains enriched in

* Corresponding author at: Department of Microbiology and Immunology, College of Biological Science, China Agricultural University, Beijing 100193, China. Tel.: +86 10 62733335; fax: +86 10 62732012.
*E-mail address:* whfeng@cau.edu.cn (W.-h. Feng).

http://dx.doi.org/10.1016/j.virol.2015.06.005
0042-6822/

sphingolipid, cholesterol, and a subclass of membrane proteins (Munro, 2003; Simons and Ikonen, 1997). Rafts can incorporate or exclude proteins selectively and coalesce into large domains to form platforms that function in many cellular processes including signal transduction, membrane trafficking, cytoskeletal organization, and pathogen infection (Brown and London, 2000; Simons and Toomre, 2000). Since lipid rafts are rich in sphingolipid and cholesterol, its resistance to cold detergent extraction has been widely used as an index (Harder et al., 1998).

Lipid rafts are utilized in the lifecycle of numerous enveloped viruses. Many enveloped viruses exploit lipid rafts for their entry stages, in which the viral enveloped glycoproteins probably insert into lipid rafts to interact with the raft-located receptors or convert from their native state to activated form to initiate or facilitate viral internalization and/or fusion (Ahn et al., 2002; Bender et al., 2003; Popik et al., 2002). Lipid rafts are also found in the intracellular structures and many special proteins such as arrays of signal transduction proteins and some viral non-structural proteins are found in lipid rafts on plasma membrane and intracellular membranes, which contribute to efficient trafficking, replication, assembly, and budding (Aizaki et al., 2004; Barman and Nayak, 2007; Bhattacharya et al., 2006; Ono and Freed, 2001). In addition, for certain viruses, the viral membrane shows similar structure to lipid raft in cell membrane, and is critical for their efficient infections (Brugger et al., 2006; Graham et al., 2003). Recently, it was reported that cholesterol-depletion drugs could inhibit PRRSV infection and influence PRRSV entry to Marc-145 cells (Huang et al., 2011). However, there is a lack of detailed and direct evidence to prove whether lipid rafts function in PRRSV entry process. Moreover, we still have little information about whether lipid rafts are required in PRRSV infection and how PRRSV utilizes lipid rafts. Here, we provide more evidence to verify that PRRSV entry is associated with lipid rafts. In addition, we show that lipid rafts in cell membrane play an important role in PRRSV replication and release, and lipid rafts in PRRSV envelope are also critical for its infection.

## Result

### *Depletion of cellular cholesterol inhibits PRRSV infection*

To assess whether PRRSV infection is sensitive to intact lipid rafts, we tested the impact of Methyl-β-cyclodextrin (MβCD), a drug widely used to sequester cholesterol (Ilangumaran and Hoessli, 1998), on the infection of different PRRSV strains. Previous studies have shown that upon treatment with MβCD membrane cholesterol levels will remain low for 9–12 h (Li et al., 2007; Rojek et al., 2008). Indeed, treatment with MβCD for 1 h effectively reduced the level of cellular cholesterol in both Marc-145 cells and PAMs by approximate 80–90% compared to that in untreated cells at the concentration of 20 mM (Fig. 1A). Moreover, 2 h following treatment with 30 mM MβCD, the Marc-145 cells or PAMs retained relative viability of 100% compared with controls (Fig. 1B), ruling out the possible nonspecific effects of cytotoxicity caused by MβCD. Next, we treated Marc-145 cells with MβCD (0, 2.5, 5, 7.5, 10, and 20 mM) for 1 h prior to infection with PRRSV strain CH1a (MOI=1), and examined PRRSV infection using indirect immunofluorescent staining and quantified PRRSV titers of the supernatant 24 h post infection. As shown in Fig. 1C and D, CH1a infection was significantly inhibited by MβCD in a dose-dependent manner. And a titer-reduction of more than $10^4$-fold was observed at the concentration of 20 mM when compared with the non-MβCD-treated cells (Fig. 1D). To investigate whether this anti-PRRSV activity is strain specific, we did the same treatment with PAMs and then infected it with HP-PRRSV strain Hpv (MOI=1). Our results showed that MβCD also inhibited Hpv infection in PAMs, and a more than 1000-fold suppression was observed at the concentration of 20 mM (Fig. 1E).

To confirm that the inhibition of PRRSV infectivity is not due to any nonspecific effect of MβCD, we performed a cholesterol reconstitution experiment (Fig. 1F). Marc-145 cells were pretreated with 10 mM MβCD for 1 h, followed by addition of cholesterol to replenish cells for 1 h. Cells were then infected with CH1a (MOI=1) and virus yield was analyzed 24 h post infection. As expected, PRRSV infection was successfully restored by cholesterol supplementation, confirming that the inhibition by MβCD is due to its specific sequestering of cholesterol. These results indicated that cellular cholesterol depletion could inhibit PRRSV infection, implicating that PRRSV infection might be associated with cellular lipid rafts.

### *Cellular cholesterol depletion inhibits PRRSV entry but has no effect on PRRSV binding*

To further explore how lipid rafts influence PRRSV infection, we first determine whether the depletion of cellular cholesterol affects PRRSV entry to the cells. The process of PRRSV entry includes early attachment and subsequent internalization. To address whether MβCD can inhibit PRRSV binding, Marc-145 cells were pretreated with MβCD and then incubated with CH1a at 4 °C (in this way, virions will bind to the cells without penetration). The level of cell-bound viral RNA was analyzed. As shown in Fig. 2A, the amount of bound virions was not affected even if a 20 mM MβCD was used. PAMs treated as above also showed little variation on their capability to bind Hpv virions (Fig. 2B). These data suggest that cholesterol depletion has no effects on virus attachment to the cells.

Previous studies have reported that PRRSV is completely internalized from the surface of Marc-145 cells within 3–6 h (Kreutz and Ackermann, 1996; Nauwynck et al., 1999). To examine whether cellular cholesterol depletion affects PRRSV internalization into Marc-145 cells, cells were pretreated with MβCD and then incubated with CH1a at 4 °C. Cells were subsequently shifted to 37 °C to allow virus internalization for 3 h and the level of internalized viral RNA in cells was analyzed (Fig. 2C). MβCD exhibited an obvious dose-dependent inhibitory effect on CH1a in Marc-145 cells, showing about 50% and 90.0% reductions of internalized PRRSV RNA in cells treated with 5 mM and 20 mM MβCD compared to that in untreated cells, respectively. A similar reduction was observed when we did the same experiment with PAMs (Fig. 2D). We also attempted to reverse the PRRSV entry by supplementing the cells with exogenous cholesterol. Marc-145 cells were pretreated with 20 mM MβCD for 1 h, followed by addition of cholesterol to replenish cells for 1 h. Then, cells were incubated with CH1a at 4 °C for 1 h and subsequently shifted to 37 °C to allow virus internalization for 3 h. Then the level of internalized viral RNA in cells was analyzed after non-internalized virions were washed away. As expected, PRRSV entry was restored by cholesterol supplementation in high concentration (Fig. 2E), confirming that the inhibition of PRRSV entry by MβCD is due to its specific sequestering of cholesterol. These observations suggest that cellular cholesterol depletion imposes an inhibition on the onset of PRRSV infection.

### *Raft-distributed receptor CD163 might contribute to the association of PRRSV glycoproteins with cellular lipid raft during entry*

Our experimental data with the cholesterol inhibitor MβCD suggest that that lipid rafts might be associated with PRRSV entry. To provide direct evidence for virion association with lipid rafts during PRRSV entry, we infected PAMs with Hpv at 4 °C for 1 h. The cells were

washed and subsequently shifted to 37 °C to initiate membrane fusion and virion penetration. Cell lysates were harvested 2 h post the temperature shift, and detergent-resistant membranes were isolated by sucrose sedimentation as described in Materials and Methods. We then performed immunoblot analysis with fractions using antibodies that are reactive to individual viral envelope proteins (Gp3, Gp4, and Gp5) (Fig. 3A). A moderate staining of Gp3 and Gp4 proteins was present in the caveolin-rich raft-fraction, indicating that PRRSV Gp3 and Gp4 enveloped proteins were associated with lipid rafts during entry. However, the protein Gp5 was almost excluded from the lipid raft fractions and recovered in non-raft fractions associated with the non-raft maker CD71 (Harder et al., 1998). However, when the PAMs were pretreated with 20 mM MβCD for 1 h, we did not succeed in isolating lipid raft and Gp3 and Gp4 were recovered in the fraction with the non-raft protein CD71 (Fig. 3B), These results suggest that lipid rafts might play a role in PRRSV entry.

It has been reported that CD163 is essential for internalization and fusion, and a functional CD163 SRCR domain 5 can interact with the Gp2 and Gp4 glycoproteins which form trimers with Gp3 (Van Gorp et al., 2010). Since the enveloped proteins of PRRSV associated with lipid rafts on plasma membrane are Gp3 and Gp4 but not Gp5, we assume that CD163 might be located in lipid raft microdomains. To verify this hypothesis, we also studied the distribution of CD163 during PRRSV entry (Fig. 3A). As expected, CD163 was found to be enriched in the raft-fractions, indicating that CD163 may be a raft-located receptor. However, it is also possible that binding of glycoproteins of PRRSV to rafts recruits CD163 to these domains from non-raft components. Thus, we next investigated whether CD163 was a raft-protein in uninfected cells. We transfected CD163 into Hela cells and then treated cells with 20 mM MβCD for 1 h at 24 h post transfection. The CD163 distribution on MβCD-treated cell membrane was compared with that of untreated cells using Immunofluorescent assay. As shown in Fig. 3C, CD163 proteins on untreated cellular membrane were speckled while these spots disappeared and changed into a uniform distribution on cellular membrane upon MβCD treatment. To

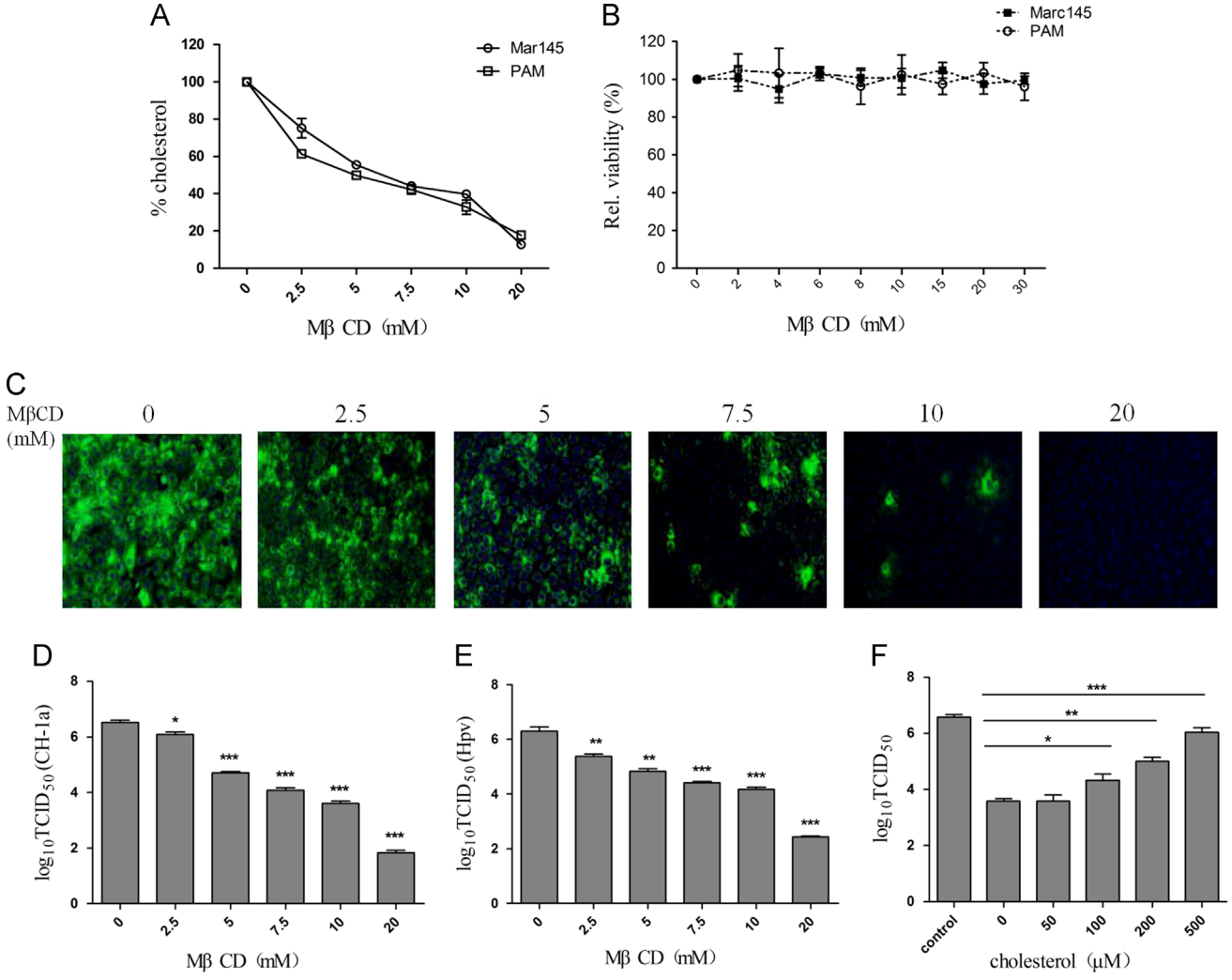


**Fig. 1.** Cellular cholesterol depletion by MβCD induced a dose-dependent anti-PRRSV activity. (A) Cholesterol levels in Marc-145 cells and PAMs treated with MβCD. Cells were treated with MβCD at the indicated concentrations for 1 h at 37 °C and then harvested for cholesterol analysis. (B) Cellular toxicity was examined in Marc-145 cells and PAMs using MTT assay and was expressed as relative cell viability compared with the viable cells in the absence of MβCD (set up as 100%). (C and D) Anti-PRRSV activity of MβCD was examined against the CH1a strain in Marc-145 cells. Marc-145 cells were pretreated with various concentrations of MβCD as described above and subsequently infected with CH1a at an MOI of 1. The infected cells were measured by indirect immunofluorescence assay for the N protein of PRRSV 24 h post-infection (C) and the virus titers ($TCID_{50}$) of supernatants were quantified (D). (E) MβCD treatment induced an antiviral activity against Hpv in PAMs. PAMs pretreated with MβCD were infected with Hpv at an MOI of 1, and then the virus titers ($TCID_{50}$) of supernatants were analyzed 24 h post infection. (F) Replenishment of cholesterol in cells rescues PRRSV infection. Marc-145 cells were treated with 10 mM MβCD for 1 h, followed by replenishment with exogenous cholesterol at the indicated concentration for 1 h. Then the cells were infected with CH1a at an MOI of 1 and the titers ($TCID_{50}$) of supernatants were measured 24 h post infection. Cells without MβCD treatment and cholesterol replenishment were set as a control. The data represent the mean ± standard deviation from three independent experiments. Significant differences compared with untreated group are denoted by * ($P < 0.05$), ** ($P < 0.01$), and *** ($P < 0.001$).

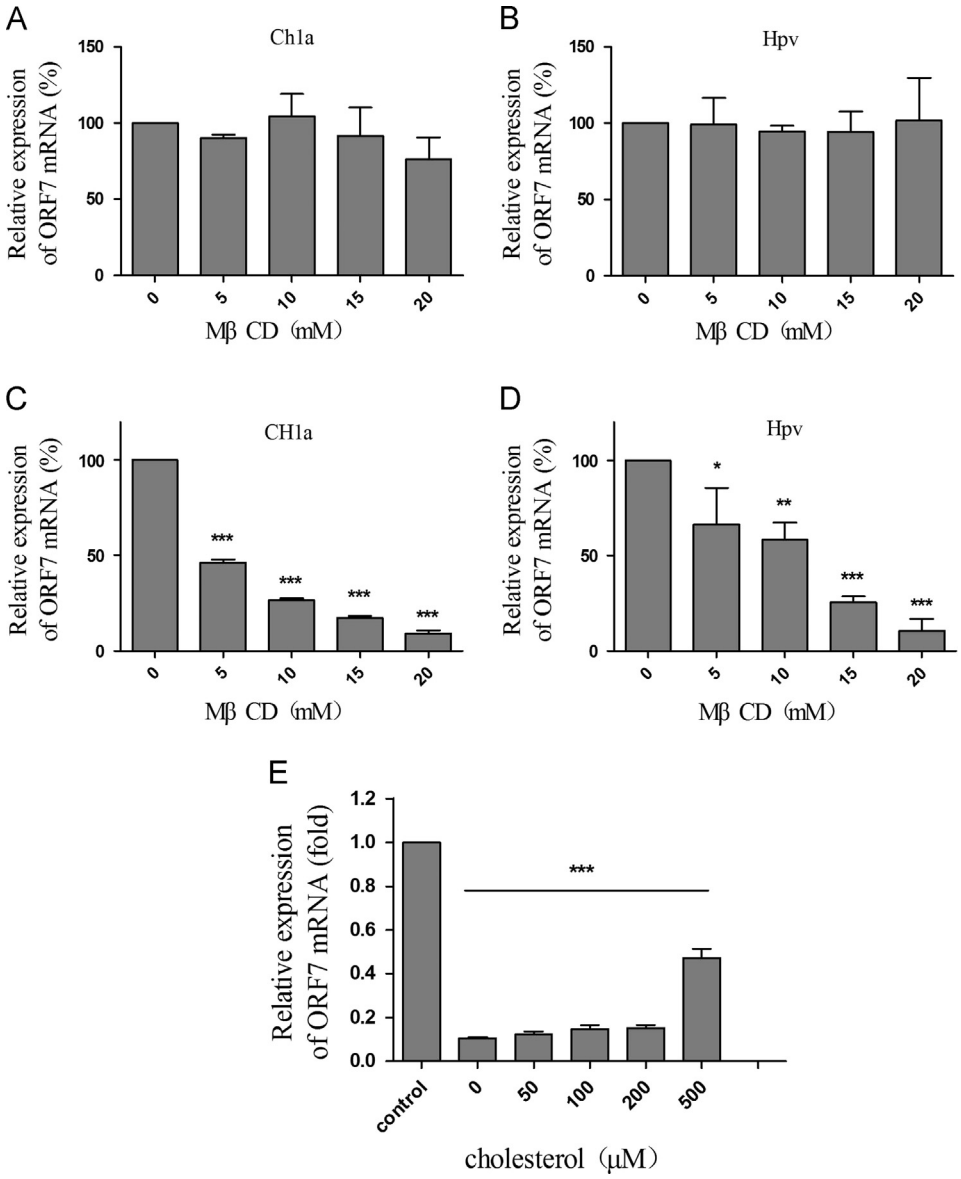


**Fig. 2.** Effect of cellular cholesterol depletion on PRRSV entry. (A and B) MβCD pretreatment of cells did not affect PRRSV binding. Marc-145 cells or PAMs were pretreated with MβCD at the indicated concentrations for 1 h at 37 °C and then incubated with CH1a (A) and Hpv (B) virions, respectively, at an MOI of 5 at 4 °C for 1 h. Unbound virus particles were removed, and the cell-associated PRRSV ORF7 RNA level was analyzed using real-time RT-PCR. (C and D) MβCD pretreatment of cells inhibited viral internalization of PRRSV. Marc-145 cells or PAMs were pretreated with MβCD at the indicated concentrations for 1 h at 37 °C prior to incubation with CH1a (C) and Hpv (D) virions at an MOI of 5 at 4 °C for 1 h. Cells were then switched to 37 °C for 3 h, followed by removal of noninternalized virions. The internalized PRRSV ORF7 RNA level in cells was analyzed using real-time RT-PCR. (E) Replenishment of cholesterol in cells rescues PRRSV entry. Marc-145 cells were treated with 20 mM MβCD for 1 h, followed by replenishment with exogenous cholesterol at the indicated concentration for 1 h. Then the cells were incubated with CH1a (MOI=5) and the internalized viral RNA level in cells was analyzed using real-time PCR. Cells without MβCD treatment and cholesterol replenishment were set as a control. The data represent the mean ± standard deviation from three independent experiments. Significant differences compared with untreated group are denoted by * ($P<0.05$), ** ($P<0.01$), and *** ($P<0.001$).

further confirm the CD163 location in uninfected PAMs, we directly used sucrose gradients to isolate detergent-insoluble fractions from PAMs and performed immunoblot to analyze CD163 in fractions (Fig. 3D). A substantial portion of CD163 was found to be restricted in the raft-fractions. These results suggest that CD163 proteins are distributed in lipid rafts on cell membrane in PAMs, which may mediate the association of PRRSV glycoproteins with rafts during viral entry.

*Lipid raft plays an important role in PRRSV replication*

RNA replication of virtually all positive-strand RNA viruses requires certain intracellular membrane structures including endoplasmic reticulums (ER), Golgi apparatus and lysosomes (Restrepo-Hartwig and Ahlquist, 1996; Shi et al., 1999; van der Meer et al., 1999). Some of these viruses induce distinct membrane structural scaffold to provide platforms for viral RNA replication, such as the formation of lipid raft associated HCV RNA replication complex (Aizaki et al., 2004; Gosert et al., 2002; Westaway et al., 1997). Therefore, we attempted to investigate whether lipid rafts are required for PRRSV RNA production. We infected PAMs with the Hpv (MOI=1) and then replaced the cell medium with fresh medium containing 10 mM MβCD 12 h later. Viral RNA levels in cells were quantitated using real-time PCR at 0, 6, and 12 h after medium switching (Fig. 4A). Compared with the PBS-treated cells, a significant reduction of the intracellular viral RNA was observed after MβCD treatment, suggesting that lipid rafts might be involved in PRRSV replication. Next, we further examined the distribution of Nsp9, the RNA dependent RNA polymerase of PRRSV after flotation analysis of PAMs which were infected with Hpv (MOI=1) for 24 h

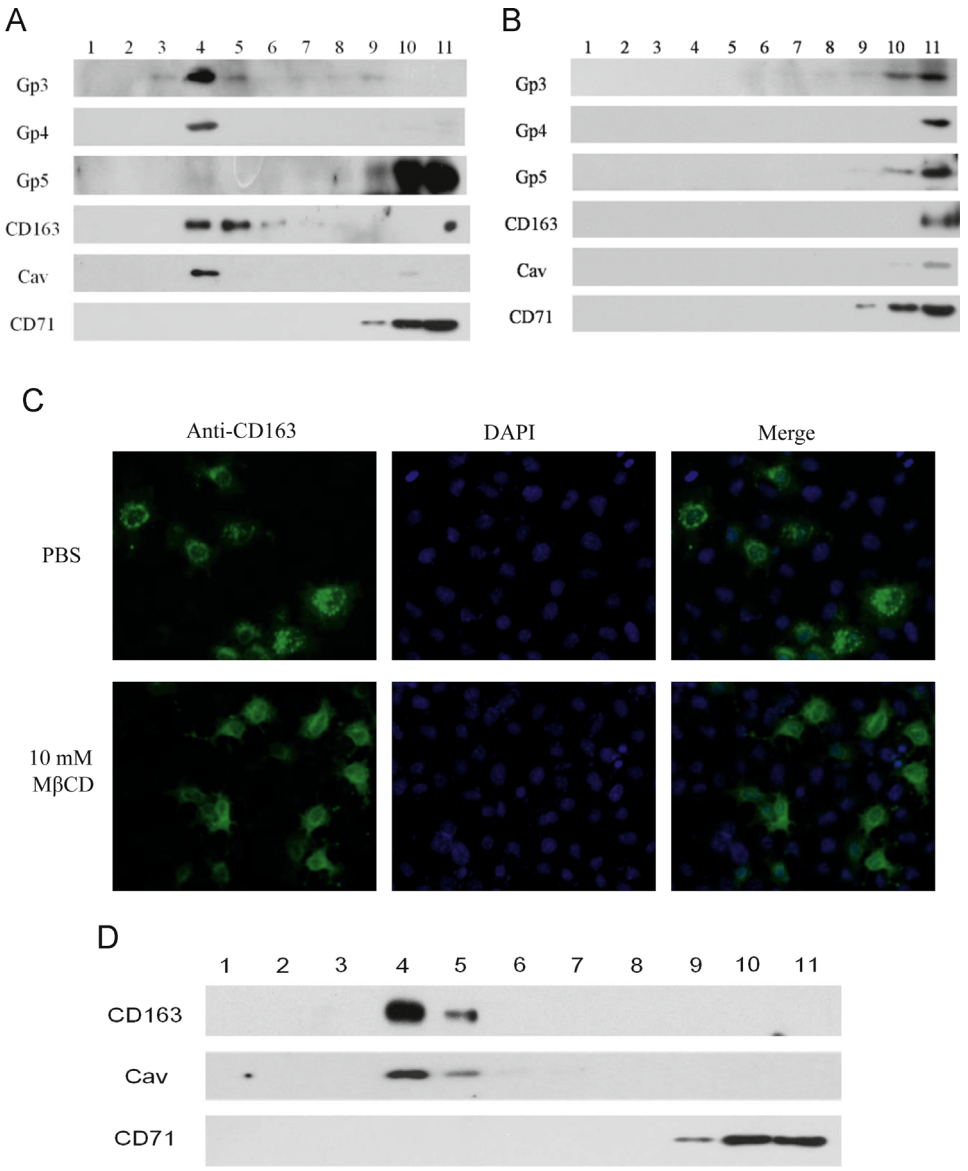


**Fig. 3.** Distribution of certain glycoproteins on the cellular lipid raft during PRRSV entry and lipid raft-location of receptor CD163. (A) The distribution of Gp3, Gp4, Gp5, and CD163 in the different sucrose gradient fractions during entry. PAMs were incubated with Hpv at an MOI of 5 at 4 °C for 1 h and then switched to 37 °C for 2 h. Cells were extracted in Triton X-100 and fractionated by discontinuous sucrose gradient centrifugation as described in Materials and Methods. The fractions were separated by SDS-12% PAGE and transferred to PVDF membranes for immunoblot analysis for nonraft marker CD71, raft maker caveolin (Cav), Gp3, Gp4, Gp5, or CD163. (B) The distribution of Gp3, Gp4, Gp5, and CD163 in different sucrose gradient fractions during PRRSV entry upon MβCD pretreatment. PAMs were pretreated with 20 mM MβCD for 1 h and then incubated with Hpv at an MOI of 5 at 4 °C for 1 h and then switched to 37 °C for 2 h. Cells were extracted in Triton X-100 and fractionated by discontinuous sucrose gradient centrifugation as described in Materials and Methods. The fractions were separated by SDS-12% PAGE and transferred to PVDF membranes for immunoblot analysis for CD71, Cav, Gp3, Gp4, Gp5, or CD163. (C) MβCD treatment affected the distribution of CD163. Hela cells were transfected with plasmid encoding CD163 and treated with 20 mM MβCD at 37 °C for 1 h at 24 h post transfection. The cells treated with PBS were set as a control. The expression of CD163 on cell membrane was stained by indirect immunofluorescence assay after MβCD treatment. (D) Association of CD163 with lipid rafts. PAMs were extracted in Triton X-100 and fractionated on sucrose gradients. Proteins were resolved on SDS-PAGE and transferred to PVDF membrane for immunoblot analysis of CD163, Cav, and CD71.

(Fig. 4B). Significantly, a substantial portion of Nsp9 was in the fraction referred to be as the lipid raft. However, when these infected PAMs were treated with 20 mM MβCD for 1 h, little lipid rafts were isolated and Nsp9 were co-recovered with CD71 (Fig. 4C). These results suggest that PRRSV RNA synthesis may occur in lipid raft membrane microdomains.

*Lipid raft disruption by cholesterol depletion enhances the production of abnormal PRRSV particles*

Lipid rafts have been reported to be implicated in the release of a wide variety of viruses, including human immunodeficiency (HIV), Newcastle disease virus (NDV) and influenza (Barman and Nayak, 2007; Laliberte et al., 2006; Nguyen and Hildreth, 2000). Thus, we attempted to investigate the effect of cholesterol depletion by MβCD treatment on PRRSV release. Marc-145 cells and PAMs were infected with CH1a and Hpv for 24 h, respectively, and then medium was replaced with fresh medium containing MβCD (0, 10, and 20 mM). At 1 h later, the amount of virus released into the medium was quantified by analysis of PRRSV envelope protein Gp5 (Fig. 5A). Our results showed that the Gp5 release was enhanced with the increasing concentration of MβCD treatment. However, the RNA level and titer of the released virus particles had no obvious difference when treated with either 10 mM or 20 mM MβCD compared to that of the no-treatment control (Fig. 5B and C). It is possible that MβCD-treatment causes the release of more

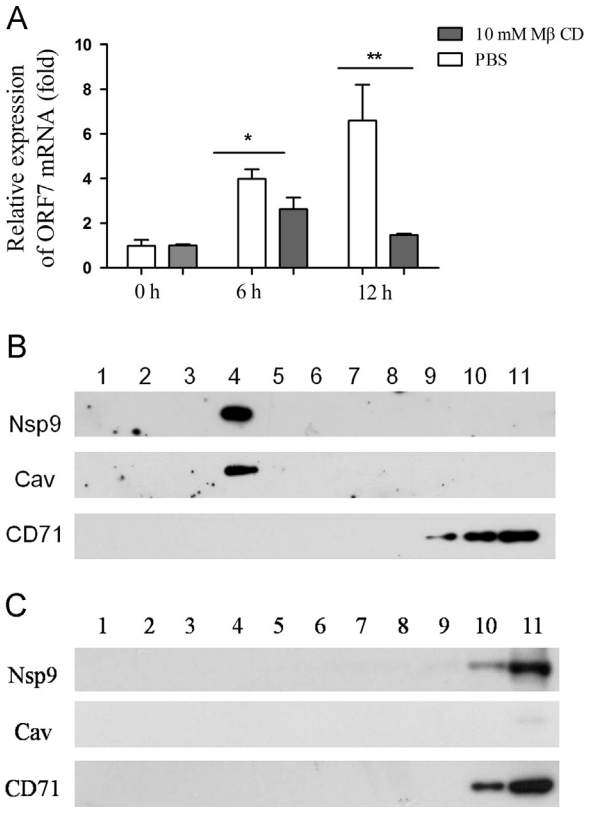


**Fig. 4.** Association of lipid raft with PRRSV replication. (A) The effect of PRRSV replication at the indicated time intervals in PAMs upon MβCD treatment. PAMs were infected with Hpv at an MOI of 1 for 12 h (represented as 0 h on graph), and then the medium was replaced with fresh medium containing 10 mM MβCD. ORF7 RNA level in cells was analyzed using real-time RT-PCR at 0, 6, and 12 h after treatment. Data shown as mean ± standard deviation from three independent experiments. Significant differences compared with 0 h group are denoted by * ($P < 0.05$) and ** ($P < 0.01$). (B) Association of Nsp9 with raft. PAMs were harvested 24 h after infection with Hpv at an MOI of 1. Cells were extracted in Triton X-100 and fractionated by discontinuous sucrose gradient centrifugation as described in Materials and Methods. Each fraction was resolved on SDS-PAGE and transferred to PVDF membrane for immunoblot analysis of Nsp9, Cav, and CD71. (C) PAMs were harvested 24 h after infection with Hpv at an MOI of 1. Cells were treated with 20 mM MβCD for 1 h and then extracted in Triton X-100 and fractionated by discontinuous sucrose gradient centrifugation as described in Materials and Methods. Each fraction was resolved on SDS-PAGE and transferred to PVDF membrane for immunoblot analysis of Nsp9, Cav, and CD71.

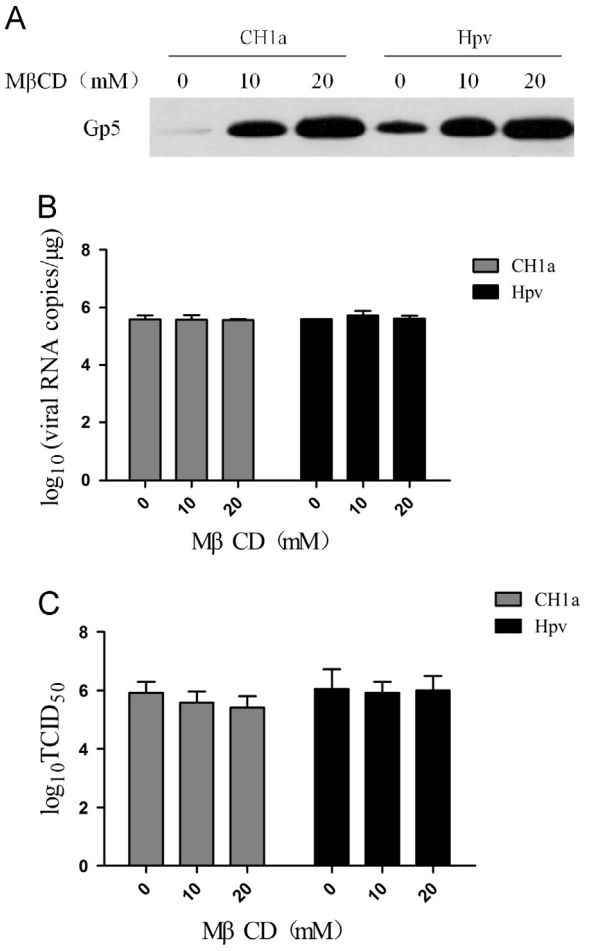


**Fig. 5.** Effect of MβCD treatment on virus release. (A) Virus particles released from MβCD-treated cells. Marc-145 cells or PAMs were infected with CH1a or Hpv at an MOI of 1. At 24 h post infection, the medium was replaced with fresh medium containing 0, 10, or 20 mM MβCD to treat cells for 1 h. The released virus particles in supernatant were harvested and viral proteins were separated in SDS-PAGE and transferred to PVDF membrane for immunoblot analysis of Gp5. (B) Viral RNA of viruses released from the infected cells after MβCD treatment was quantified by real-time RT-PCR. (C) Titers ($TCID_{50}$) of viruses released from the infected cells after MβCD treatment were quantified. Data shown as mean ± standard deviation from three independent experiments.

immature viral particles from infected cells compared with that in untreated infected cells. There is also a possibility that MβCD-treatment changed the virion components of the released PRRSV particles.

### *Depletion of cholesterol from the viral envelope impairs PRRSV infection*

To clarify whether cholesterol elimination of virions affects PRRSV infectivity, we depleted cholesterol of CH1a and Hpv virions by MβCD treatment prior to infection. Purified PRRSV were treated with 0, 10, 20, 30, 50, or 80 mM MβCD for 1 h at 37 °C, and then the drug was removed by ultracentrifugation as described in Materials and Methods. The residual cholesterol content in viral preparations was measured after MβCD treatment. As shown in Fig. 6A, both the envelopes of CH1a and Hpv virions contained a certain amount of cholesterol and a remarkable dose-dependent decline was observed after MβCD treatment (approximately 90.0% at 80 mM MβCD). Then, we used MβCD-treated CH1a virions to infect Marc-145 cells and examined the infected cells using an indirect immunofluorescent assay 24 h post infection. As shown in Fig. 6B, a significant dose-dependent reduction was observed for the number of infected cells. We also analyzed the direct effects of MβCD treatment on the titers of CH1a and Hpv virions. MβCD induced a significant dose-dependent titer-reduction for CH1a, and a more than $10^6$-fold reduction was observed at the concentration of 80 mM compared with the untreated virus (Fig. 6C). Similarly, MβCD treatment induced a more than $10^4$-fold reduction for the titer of Hpv at the concentration of 80 mM when compared with the untreated virus (Fig. 6D).

To further verify that the decrease in PRRSV infectivity is caused by cholesterol depletion in the virus envelope, we attempted to reverse the infectivity by supplementing virions with exogenous cholesterol. After extraction of viral cholesterol in CH1a by 20 mM MβCD for 1 h, virus was supplemented with exogenous cholesterol (0, 50, 100, 200, and 500 μM) for 30 min at 37 °C, and then the titer of the virus was tested. The infectivity of MβCD-treated virus particles was recovered upon cholesterol replenishment in a dose-dependent manner, even though it was not completely restored up to 500 μM cholesterol (Fig. 6E). These data suggest that the effect of MβCD on PRRSV infectivity is mainly due to the reduced cholesterol levels in the virus envelope and the

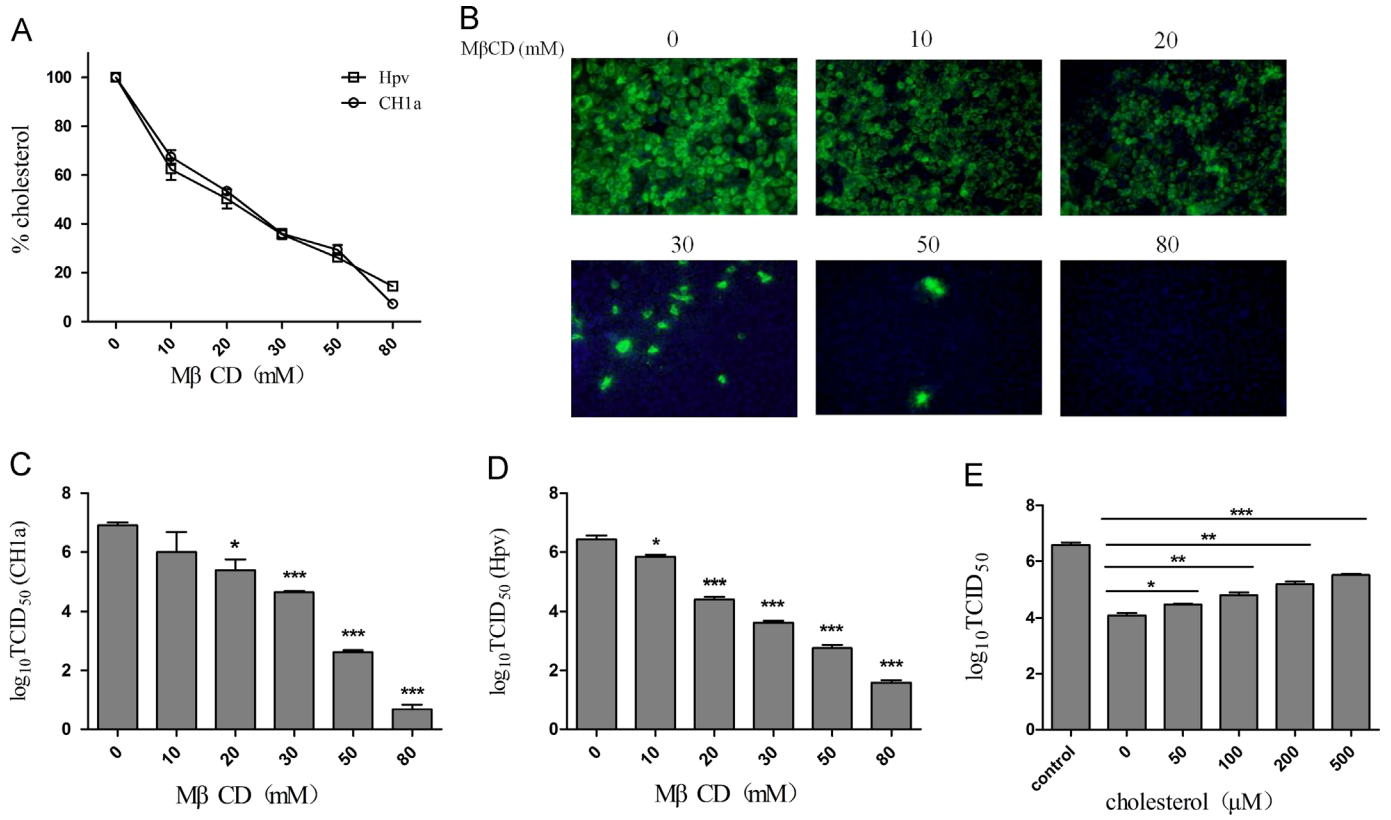


**Fig. 6.** Requirement of cholesterol in the viral envelope for efficient PRRSV infection. Purified virus was treated with 0, 10, 20, 30, 50, and 80 mM MβCD for 1 h at 37 °C and then re-collected as described in Materials and Methods. (A) Residual cholesterol in virions following MβCD treatment was quantitated. (B) Cholesterol depletion of virus inhibited PRRSV infection in Marc-145 cells. Marc-145 cells were incubated with MβCD-treated CH1a virions as above. The infected cells were stained by indirect immunofluorescence assay for the PRRSV N protein 24 h post-infection. (C and D) The titers ($TCID_{50}$) of CH1a (C) and Hpv (D) treated with various concentrations of MβCD as above were quantified. (E) Infection efficiency of cholesterol-depleted PRRSV after replenishment with exogenous cholesterol. CH1a virions were cholesterol depleted by treatment with 20 mM MβCD at 37 °C for 1 h. Prior to infection in Marc-145 cells, virions were replenished by increasing concentrations of exogenous cholesterol at 37 °C for 30 min. Infection efficiencies were determined by analysis of the viral titer ($TCID_{50}$). The data represent the mean ± standard deviation from three independent experiments. Significant differences compared with untreated group are denoted by * ($P < 0.05$), ** ($P < 0.01$), and *** ($P < 0.001$).

infection of PRRSV to target cells is dependent on the integrity of the lipid raft in the virus envelope.

### *Depletion of cholesterol from the PRRSV envelope results in permeabilization of virions*

Since our data show that the cholesterol reduction in viral envelope can inhibit PRRSV infectivity, it is possible that viral lipid raft disruption induced by cholesterol removal disrupts PRRSV virus particles. To extend our understanding of this effect, purified CH1a virions were treated with 0, 10, 20, 30, 50, or 80 mM MβCD for 1 h at 37 °C and re-purified by ultracentrifugation as described in Materials and Methods. Western blotting was then performed to determine whether MβCD treatment has effects on viral envelope protein (Gp5) or Nucleocapsid protein (N protein). As shown in Fig. 7A, the amount of N protein exhibited a dose-dependent reduction induced by MβCD treatment, while the amount of Gp5 was fairly constant up to 80 mM MβCD. The permeabilization was defined as a greater decrease of the capsid protein relative to the envelope glycoprotein. Thus, depletion of cholesterol from viral envelope resulted in permeabilization of PRRSV virions. We also tested the viral RNA levels of the MβCD-treated CH1a virions to determine whether viral RNA is retained in PRRSV virions (Fig. 7B). Our results showed little change in the amount of viral RNA in CH1a virions after MβCD treatment, suggesting that PRRSV particles do not lose viral RNA after permeabilization by MβCD. These results reveal that depletion of

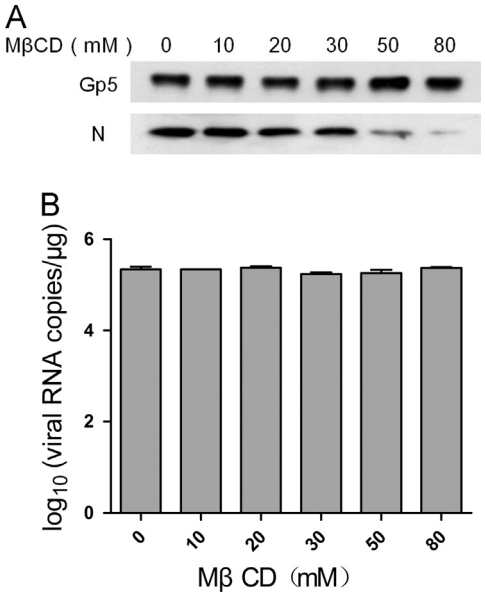


**Fig. 7.** Effect of PRRSV particles with MβCD treatment. (A) Treatment of PRRSV with increasing concentrations of MβCD resulted in permeabilization of the viral membrane and loss of capsid protein. CH1a virions were treated with MβCD at the indicated concentration for 1 h at 37 °C and re-collected. Samples were analyzed by SDS-PAGE and transferred to PVDF membrane for immunoblot analysis of Gp5 and N protein. (B) Viral RNA retained upon permeabilization induced by MβCD treatment. Virus prepared as above was analyzed for particle-associated viral RNA by real-time RT-PCR. Virus input was normalized to Gp5 content.

viral cholesterol may impair PRRSV infectivity due to the virion disruption and leak of nucleocapsid protein.

## Discussion

Lipid rafts exist in cell plasma membranes, intracellular organelles and viral envelopes, which are different in their composition, physical properties, and biological functions (Brown and London, 1998; Chazal and Gerlier, 2003; Ikonen, 2001). The significance of lipid rafts in either the viral envelope or the target cell membrane has been demonstrated for many viruses. Here, we investigated the importance of lipid rafts in viral envelope and cellular membranes for PRRSV infection.

Our work showed that cellular cholesterol was important in establishing PRRSV infection both in Marc-145 cells and PAMs. By incubating cells with cholesterol-depletion drug before virus infection, only cellular cholesterol will be removed, allowing viral cholesterol and infectivity to remain intact. Under such condition, the efficiency of infection is dependent on the amount of cholesterol residual on cell membrane. Direct replenishment of exogenous cholesterol to cells after drug-mediated cholesterol depletion substantially restored PRRSV infection. These data indicate that the efficiency of PRRSV infection at least in part is associated with the cholesterol level on cell membranes.

Molecular simulations of model membranes show that the integrity of lipid raft microdomains is sensitive to minor changes of cholesterol (Risselada and Marrink, 2008). Thus, cholesterol is a major component of lipid raft microdomains, and manipulation of cholesterol present within membranes is frequently used to implicate lipid rafts. Therefore, we further investigated whether and how PRRSV infection was affected by cellular lipid rafts. PRRSV entry process is mediated by receptor-specific endocytosis, where the virus attachment, internalization and membrane fusion occur sequentially (Nauwynck et al., 1999). Previous study has reported the significant suppression of cellular cholesterol depletion on PRRSV entry, which is in consistent with our results (Sun et al., 2011). These results are similar to the findings observed on some other members of the order Nidovirales such as HCoV-229E, MHV and SARS-CoV (Choi et al., 2005; Li et al., 2007; Nomura et al., 2004; Thorp and Gallagher, 2004). However, how lipid rafts contribute to PRRSV entry is not explicit, Although it has been reported that Gp4 is located in lipid rafts when it is exogenously expressed in HeLa cells and that Gp4 and CD163 co-located in lipid rafts in a porcine kidney cell line (Du et al., 2012), there is no direct and convincing evidence to show the association of Gp4, CD163, and other glycoproteins with lipid rafts in PAMs during PRRSV entry. By the use of Triton X-100 extract and discontinuous sucrose gradient fractionation, we showed that the viral envelope proteins Gp3 and Gp4, but not Gp5, were partitioned in lipid rafts during virus penetration of PAMs. These results correspond well with their roles in PRRSV entry. Gp5 interacts with the sialoadhesin receptor to mediate virus-cell binding and initial endocytosis (Van Breedam et al., 2010b), while Gp3 and Gp4, which form trimers with Gp2, interacting with CD163 are essential for the following internalization and fusion (Van Gorp et al., 2010). These data imply that lipid rafts probably utilize cellular receptor CD163 to mediate its association with PRRSV envelope proteins during entry. Consistent with this assumption, we showed that CD163 was mainly located in lipid raft microdomain of PAM membrane, and the distribution of the CD163 on cell membrane was found to be altered by cholesterol depletion. Moreover, PRRSV enters cells by a process of clathrin-mediated endocytosis which is distinguished from lipid raft-mediated endocytosis pathway (Kreutz and Ackermann, 1996; Mercer et al., 2010; Nauwynck et al., 1999). Therefore, we infer that lipid rafts probably contribute to membrane fusion but not endocytosis in PRRSV entry. The glycoproteins–receptor interaction may trigger the raft clustering to form platforms, which may function in PRRSV membrane fusion.

Viral RNA replication is a multistep process involving a replication complex that is formed by viral and cellular components with the viral genomic RNA template. This replication complex is embedded within particular virus-induced membrane vesicles, which serve as the anchoring sites for the PRRSV replication complex to mediate migration of the replication complex between cellular organelles (Bost et al., 2003; den Boon and Ahlquist, 2010; Netherton and Wileman, 2011). In the present study, a significant reduction of the intracellular viral RNA resulted from cholesterol depletion, indicating that lipid rafts are probably involved in PRRSV RNA production. PRRSV replication is directed by at least 14 replicase proteins that have both common enzymatic activities, especially the viral RNA-dependent RNA polymerase Nsp9 (Fang and Snijder, 2010; Yun and Lee, 2013). Flotation analysis of infected PAMs showed that Nsp9 was distributed in lipid raft fractions. Thus, lipid rafts might serve as the sites for viral RNA replication complex anchored to PRRSV-induced special membrane structural scaffold. However, the precise mechanism for this association of special membrane structure with viral replication complex remains to be determined. Membrane lipid rafts have been implicated in the assembly and release of many enveloped viruses. Our results also showed that lipid raft disruption increased the release of PRRSV particles. For some virus such as influenza virus, lipid rafts and their underlying cortical cytoskeleton probably provide a framework for specific and ordered viral protein-protein interactions required for proper assembly (Roberts and Compans, 1998; Simpson-Holley et al., 2002). Cholesterol depletion could induce rearrangement of the cortical actin cytoskeleton in many cells and cortical actin rearrangements also could induce reorganization of lipid raft microdomains (Chadda et al., 2007; Francis et al., 1999; Simpson-Holley et al., 2002). Therefore, perturbation of actin cytoskeleton caused by cholesterol depletion might contribute to the enhanced release of PRRSV particles envelope proteins. However, no increase in viral RNA level or virus infectivity was observed for the PRRSV particles released from lipid raft disrupted cells. It is possible that lipid raft disruption might induce abnormal assembly and release of PRRSV particles.

Cholesterol depletion may also mediate disruption of PRRSV particles and directly cause the reduction in viral infectivity. PRRSV virions contain a certain amount of cholesterol and this lipid feature seems to be critical in sustaining its integrity. Our results showed that both CH1a and Hpv infectivity was decreased in a dose-dependent manner when the viruses were treated with cholesterol-depletion drug. Measuring the residual cholesterol in PRRSV virions exposed to increasing concentrations of MβCD indicated that the loss of infectivity was closely associated with reduction in virion cholesterol. The loss of viral infectivity after cholesterol depletion is likely due to partly structure destruction such as loss of viral structure proteins or loss of viral RNA. Indeed, PRRSV viral envelopes were permeabilized when treated with MβCD at a high concentration, evidenced by the loss of PRRSV nucleoprotein (N). Accordingly, we were unable to completely restore virus infectivity by adding back cholesterol to permeabilized virions. Presumably, even though the large holes in the viral membrane can be repaired by cholesterol, patching the membrane probably cannot overcome the loss of critical viral proteins. Recent cryo-electron tomographic structure determination of PRRSV has provided a possible model for the nucleocapsid–RNA organization in the virion. This model speculates that two layers of N dimers form a linked, twisted chain with the RNA in the middle, and this chain is then bundled into a roughly spherical shape that leaves a hollow interior (Dokland, 2010; Spilman et al., 2009). The disordered appearance of the PRRSV core may suggest a more loosely organized nucleocapsid which makes it

easier for the N protein to leak upon MβCD treatment. However, the permeabilization of PRRSV virions may not be enough to result in the loss of the entire genome. Therefore, disassembly of lipid rafts on the virus envelope affected integrity of viral envelope and caused the viral envelope leakage of viral proteins to adversely affect virus infectivity.

In summary, our results have shown that PRRSV infection depends on the presence of lipid rafts in both cellular membrane and viral envelope. Cellular lipid rafts play an essential role in PRRSV entry, replication and release, and viral lipid raft structures are required to maintain virion core integrity to ensure PRRSV infectivity. These findings promote us to further investigate how viral proteins are associated with lipid rafts and how lipid raft domains function in the organization of a mature PRRSV particle production. Also, the perturbation of membrane lipid rafts by small molecules to interfere with PRRSV infection could provide a means for development of antiviral agents.

## Materials and methods

### *Cells and viruses*

Marc-145 cells and Hela cells were maintained in Dulbecco's minimum essential medium (DMEM) supplemented with 10% FBS. Porcine alveolar macrophages (PAMs) were obtained from post-mortem lung lavage of 8-week-old specific pathogen free (SPF) pigs, and maintained in RPMI 1640 medium with 10% FBS. All the cells were cultured and maintained at 37 °C with 5% $CO_2$. PRRSV strains, CH1a (a type 2 PRRSV strain isolated in China) and Hpv (a highly pathogenic PRRSV (HP-PRRSV) isolate), were propagated and titrated in Marc-145 cells and PAMs. Briefly, PRRSV was serially diluted 10-fold in complete DMEM or RPMI 1640 to infect $5 \times 10^4$ Marc-145 cells or PAMs in 96-well plates. PRRSV infection was determined 48 h post infection using immunofluorescent staining for the PRRSV N protein. The viral titer was determined by the Reed-Muench method and expressed as tissue culture infective dose 50% ($TCID_{50}$).

### *Antibodies and reagents*

Methyl-β-cyclodextrin (MβCD) was from Sigma-Aldrich. Antibody against caveolin-1 was purchased from Cell Signaling Technology. Anti-CD71 antibody was purchased from Acris Antibodies GmbH. Anti-PRRSV N protein monoclonal antibody was purchased from Rural Technologies. Anti-Gp3 antibody was a gift from Dr. Zhi-jun Tian (Harbin Veterinary Research Institute, CAAS, China). The antisera for Gp4, Gp5, and Nsp9 were prepared by our lab. Antibody against CD163 was purchased from AbD Serotec Company. Goat anti-mouse or anti-rabbit IgG secondary antibodies were also purchased from Santa Cruz. Goat anti-porcine IgG secondary antibody was purchased from Bethyl Laboratories. Rabbit anti-goat IgG secondary antibody was purchased from EASYBIO Company.

### *Plasmid*

The cDNA encoding porcine CD163 was amplified using reverse transcription-PCR (RT-PCR) from total RNAs extracted from porcine alveolar macrophages (PAMs) and cloned into pcDNA3.1.

### *Cholesterol measurement*

Cholesterol was measured using an Amplex Red cholesterol assay kit (Molecular Probes, Eugene, Oreg.) following the manufacturer's introduction.

### *Cell viability assay*

Cytotoxic effects of MβCD were evaluated by the MTT (3-(4,5)-dimethylthiahiazo(-z-y1)-3,5-di-phenytetrazolimromide) assay. Marc-145 cells or PAMs in a 96-well plate were cultured in 100 μl DMEM or RPMI 1640 containing 0, 2, 4, 6, 8, 10, 15, 20, or 30 mM MβCD for 2 h at 37 °C. Next, the culture medium was replaced with fresh medium containing 20 μl of 5 mg/ml MTT after washing three times with PBS, and cells were further cultured for 4 h at 37 °C. Cells were then washed carefully and 150 μl DMSO was added per well to dissolve the crystals for 10 min. The resulting absorbance of each well was recorded at 490 nm using a plate reader.

### *Indirect immunofluorescent assay*

Cells were fixed with methanol–acetone solution (1:1) for 10 min at 4 °C, and then were blocked with 5% goat serum in PBS for 30 min at 37 °C. PRRSV N protein or CD163 was detected using corresponding specific monoclonal antibody, MAb SDOW17 (1:10,000; Rural Technologies) or MAb MCA2311 (1:5000; AbD Serotec), and the secondary goat anti-mouse IgG (H+L) conjugated with FITC (1:200, Jackson ImmunoResearch). Nuclei were stained with 4, 6-diamidino-2-phenylindole (DAPI). Immunofluorescence was observed using Leica Microsystems CMS GmbH.

### *PRRSV binding and internalization assay*

For binding assay, Marc-145 cells or PAMs were pretreated with MβCD (0, 5, 10, 15, and 20 mM) for 1 h and then incubated with CH1a (MOI=5) or Hpv (MOI=5) at 4 °C for 1 h. Then, the unbound viruses in supernatants were removed and the level of cell-bound viral RNA was analyzed by real-time PCR. For entry assay, Marc-145 cells or PAMs were pretreated with MβCD (0, 5, 10, 15, and 20 mM) for 1 h and then incubated with CH1a (MOI=5) or Hpv (MOI=5) at 4 °C for 1 h. The inoculums were replaced with fresh culture medium to eliminate the unbound virus particles and cells were subsequently shifted to 37 °C to allow virus internalization for 3 h. Then cells were carefully washed with phosphate buffered saline (PBS) three times to remove the noninternalized virions and the level of viral RNA in cells was analyzed using real-time PCR.

### *Quantitation of viral RNA*

The RNA of purified virus was extracted with the viral RNA kit (OMEGA). Total RNA from Marc-145 cells or PAMs was extracted using the TRIzol reagent. RNAs were converted to cDNA using Superscript III Reverse Transcriptase (Invitrogen). For the quantification of purified virus, PRRSV RNA was analyzed using quantitative real-time RT-PCR with primers designed against PRRSV ORF7 (Patel et al., 2008). A plasmid containing ORF7 sequence was used to generate a standard curve, and RNA copies in all samples were calculated based on it (Han et al., 2009). The transcript levels of cell-associated viral RNA were relatively quantified by the 2-ΔΔCT Method (Livak and Schmittgen, 2001). glyceraldehyde-3-phosphate dehydrogenase (GAPDH) mRNA was set as a control.

### *Lipid raft isolation*

Low-density detergent-insoluble lipid raft fractions were isolated as described previously with modifications (Chung et al., 2005). Briefly, PAMs were scraped with a rubber policeman into ice-cold PBS and collected by centrifugation at 1000*g* for 3 min at 4 °C. Then pelleted cells were lysed using 0.3 ml of ice-cold TNE buffer (25 mM Tris [pH 7.5], 150 mM NaCl, 5 mM EDTA) containing

1% Triton X-100 (Merck), 1 mM NaF, and a cocktail of protease inhibitors (Thermo) at 4 °C for 30 min with gentle agitation. Then, the cell lysates were centrifuged at 4 °C for 10 min at 3500*g* to remove nuclei and insoluble materials. The supernatants were collected and mixed with equal volumes of 80% (wt/vol) sucrose in TNE buffer and then placed in the bottoms of ultracentrifuge tubes. A discontinuous sucrose gradient was formed by sequentially overlaying 2.1 ml of 30% and 1.2 ml of 5% sucrose in TNE buffer. These mixtures were centrifuged at 4 °C for 18 h at 250,000*g* in a SW 55 Ti rotor (Beckman). After centrifugation, lipid rafts could be visible as an opaque band at the boundary between the 5% and 30% sucrose solutions. A total of 11 gradient fractions were collected from the top to bottom and stored at −80 °C until use.

### *Purification of virus and preparation of MβCD-treated virus*

Culture supernatants were clarified by centrifugation at 2500*g* for 5 min and then viruses were isolated from clarified cell culture supernatants subjected to sedimentation through 20% sucrose (wt/vol) to 65% sucrose interface by centrifuging at 4 °C for 10 h at 100,000*g* in a SW50.1 rotor (Beckman). After virion flotation, purified virus was taken from 20% to 65% sucrose interface fractions and stored at −80 °C until use.

MβCD-treated virus was prepared by incubating virus in the presence of the indicated concentration of MβCD for 1 h at 37 °C with gentle mixing. Virus was then re-purified by ultracentrifugation at 4 °C for 2 h at 200,000*g* in a SW 55 Ti rotor (Beckman). The resulting pellet obtained for each treatment condition was re-suspended to the same volume of PBS. Treated and concentrated virus was divided into aliquots in small volumes and stored at −80 °C until use.

### *Western blot analysis*

Similar amount of volume from each sample was resolved by SDS-PAGE and transferred to polyvinylidene difluoride (PVDF) membranes (Millipore). Membranes were blocked with 5% nonfat milk in phosphate-buffered saline with 0.05% Tween 20 (PBST) and incubated for 2 h at room temperature with the primary antibodies at a suitable dilution (anti-Gp3 and –Gp4 at 1:200, anti-CD71 at 1:500, anti-caveolin at 1:1000, anti-N protein at 1:2000, anti-Nsp9 at 1:3000, and anti-Gp5 and –CD163 at 1:5000). The membranes were washed by PBST and then incubated with the appropriate secondary antibody for 1 h at a dilution of 1:10,000. The membranes were washed by PBST again and the antibodies were visualized by use of the enhanced chemiluminescence (ECL) reagent according to the manufacturer's instructions.

### *Statistical analysis*

All experiments were performed with at least three independent replicates. Results were analyzed by GraphPad Prism software using Student's *t* test. $P < 0.05$ was considered to be statistically significant.

## Acknowledgments

This work was supported by the State Key Laboratory of Agrobiotechnology, China Agricultural University, China (Grant 2013SKLAB1-5 and 2014SKLAB1-3), and the Research Fund for the Doctoral Program of Higher Education of China (Grant no. 20130008110028).

## References

Ahn, A., Gibbons, D.L., Kielian, M., 2002. The fusion peptide of Semliki Forest virus associates with sterol-rich membrane domains. J. Virol. 76 (7), 3267–3275.
Aizaki, H., Lee, K.J., Sung, V.M., Ishiko, H., Lai, M.M., 2004. Characterization of the hepatitis C virus RNA replication complex associated with lipid rafts. Virology 324 (2), 450–461.
Barman, S., Nayak, D.P., 2007. Lipid raft disruption by cholesterol depletion enhances influenza A virus budding from MDCK cells. J. Virol. 81 (22), 12169–12178.
Bender, F.C., Whitbeck, J.C., Ponce de Leon, M., Lou, H., Eisenberg, R.J., Cohen, G.H., 2003. Specific association of glycoprotein B with lipid rafts during herpes simplex virus entry. J. Virol. 77 (17), 9542–9552.
Bhattacharya, J., Repik, A., Clapham, P.R., 2006. Gag regulates association of human immunodeficiency virus type 1 envelope with detergent-resistant membranes. J. Virol. 80 (11), 5292–5300.
Bost, A.G., Venable, D., Liu, L., Heinz, B.A., 2003. Cytoskeletal requirements for hepatitis C virus (HCV) RNA synthesis in the HCV replicon cell culture system. J. Virol. 77 (7), 4401–4408.
Brown, D.A., London, E., 1998. Functions of lipid rafts in biological membranes. Annu. Rev. Cell Dev. Biol. 14, 111–136.
Brown, D.A., London, E., 2000. Structure and function of sphingolipid- and cholesterol-rich membrane rafts. J. Biol. Chem. 275 (23), 17221–17224.
Brugger, B., Glass, B., Haberkant, P., Leibrecht, I., Wieland, F.T., Krausslich, H.G., 2006. The HIV lipidome: a raft with an unusual composition. Proc. Natl. Acad. Sci. USA 103 (8), 2641–2646.
Calvert, J.G., Slade, D.E., Shields, S.L., Jolie, R., Mannan, R.M., Ankenbauer, R.G., Welch, S.K., 2007. CD163 expression confers susceptibility to porcine reproductive and respiratory syndrome viruses. J. Virol. 81 (14), 7371–7379.
Chadda, R., Howes, M.T., Plowman, S.J., Hancock, J.F., Parton, R.G., Mayor, S., 2007. Cholesterol-sensitive Cdc42 activation regulates actin polymerization for endocytosis via the GEEC pathway. Traffic 8 (6), 702–717.
Chazal, N., Gerlier, D., 2003. Virus entry, assembly, budding, and membrane rafts. Microbiol. Mol. Biol. Rev. 67 (2), 226–237 (table of contents).
Choi, K.S., Aizaki, H., Lai, M.M., 2005. Murine coronavirus requires lipid rafts for virus entry and cell–cell fusion but not for virus release. J. Virol. 79 (15), 9862–9871.
Chung, C.S., Huang, C.Y., Chang, W., 2005. Vaccinia virus penetration requires cholesterol and results in specific viral envelope proteins associated with lipid rafts. J. Virol. 79 (3), 1623–1634.
Collins, J.E., Benfield, D.A., Christianson, W.T., Harris, L., Hennings, J.C., Shaw, D.P., Goyal, S.M., McCullough, S., Morrison, R.B., Joo, H.S., et al., 1992. Isolation of swine infertility and respiratory syndrome virus (isolate ATCC VR-2332) in North America and experimental reproduction of the disease in gnotobiotic pigs. J. Vet. Diagn. Invest. 4 (2), 117–126.
Conzelmann, K.K., Visser, N., Van Woensel, P., Thiel, H.J., 1993. Molecular characterization of porcine reproductive and respiratory syndrome virus, a member of the arterivirus group. Virology 193 (1), 329–339.
Dea, S., Gagnon, C.A., Mardassi, H., Pirzadeh, B., Rogan, D., 2000. Current knowledge on the structural proteins of porcine reproductive and respiratory syndrome (PRRS) virus: comparison of the North American and European isolates. Arch. Virol. 145 (4), 659–688.
den Boon, J.A., Ahlquist, P., 2010. Organelle-like membrane compartmentalization of positive-strand RNA virus replication factories. Annu. Rev. Microbiol. 64, 241–256.
Dokland, T., 2010. The structural biology of PRRSV. Virus Res. 154 (1–2), 86–97.
Du, Y., Pattnaik, A.K., Song, C., Yoo, D., Li, G., 2012. Glycosyl-phosphatidylinositol (GPI)-anchored membrane association of the porcine reproductive and respiratory syndrome virus GP4 glycoprotein and its co-localization with CD163 in lipid rafts. Virology 424 (1), 18–32.
Duan, X., Nauwynck, H.J., Pensaert, M.B., 1997. Effects of origin and state of differentiation and activation of monocytes/macrophages on their susceptibility to porcine reproductive and respiratory syndrome virus (PRRSV). Arch. Virol. 142 (12), 2483–2497.
Fang, Y., Snijder, E.J., 2010. The PRRSV replicase: exploring the multifunctionality of an intriguing set of nonstructural proteins. Virus Res. 154 (1–2), 61–76.
Fang, Y., Treffers, E.E., Li, Y., Tas, A., Sun, Z., van der Meer, Y., de Ru, A.H., van Veelen, P.A., Atkins, J.F., Snijder, E.J., Firth, A.E., 2012. Efficient -2 frameshifting by mammalian ribosomes to synthesize an additional arterivirus protein. Proc. Natl. Acad. Sci. USA 109 (43), E2920–E2928.
Forsberg, R., 2005. Divergence time of porcine reproductive and respiratory syndrome virus subtypes. Mol. Biol. Evol. 22 (11), 2131–2134.
Francis, S.A., Kelly, J.M., McCormack, J., Rogers, R.A., Lai, J., Schneeberger, E.E., Lynch, R.D., 1999. Rapid reduction of MDCK cell cholesterol by methyl-beta-cyclodextrin alters steady state transepithelial electrical resistance. Eur. J. Cell Biol. 78 (7), 473–484.
Gosert, R., Kanjanahaluethai, A., Egger, D., Bienz, K., Baker, S.C., 2002. RNA replication of mouse hepatitis virus takes place at double-membrane vesicles. J. Virol. 76 (8), 3697–3708.
Graham, D.R., Chertova, E., Hilburn, J.M., Arthur, L.O., Hildreth, J.E., 2003. Cholesterol depletion of human immunodeficiency virus type 1 and simian immunodeficiency virus with beta-cyclodextrin inactivates and permeabilizes the virions: evidence for virion-associated lipid rafts. J. Virol. 77 (15), 8237–8248.

Han, X., Fan, S., Patel, D., Zhang, Y.J., 2009. Enhanced inhibition of porcine reproductive and respiratory syndrome virus replication by combination of morpholino oligomers. Antiviral Res. 82 (1), 59–66.
Hanada, K., Suzuki, Y., Nakane, T., Hirose, O., Gojobori, T., 2005. The origin and evolution of porcine reproductive and respiratory syndrome viruses. Mol. Biol. Evol. 22 (4), 1024–1031.
Harder, T., Scheiffele, P., Verkade, P., Simons, K., 1998. Lipid domain structure of the plasma membrane revealed by patching of membrane components. J. Cell Biol. 141 (4), 929–942.
Huang, L., Zhang, Y.P., Yu, Y.L., Sun, M.X., Li, C., Chen, P.Y., Mao, X., 2011. Role of lipid rafts in porcine reproductive and respiratory syndrome virus infection in MARC-145 cells. Biochem. Biophys. Res. Commun. 414 (3), 545–550.
Ikonen, E., 2001. Roles of lipid rafts in membrane transport. Curr. Opin. Cell Biol. 13 (4), 470–477.
Ilangumaran, S., Hoessli, D.C., 1998. Effects of cholesterol depletion by cyclodextrin on the sphingolipid microdomains of the plasma membrane. Biochem. J. 335 (Pt 2), 433–440.
Johnson, C.R., Griggs, T.F., Gnanandarajah, J., Murtaugh, M.P., 2011. Novel structural protein in porcine reproductive and respiratory syndrome virus encoded by an alternative ORF5 present in all arteriviruses. J. Gen. Virol. 92 (Pt 5), 1107–1116.
Kim, H.S., Kwang, J., Yoon, I.J., Joo, H.S., Frey, M.L., 1993. Enhanced replication of porcine reproductive and respiratory syndrome (PRRS) virus in a homogeneous subpopulation of MA-104 cell line. Arch. Virol. 133 (3–4), 477–483.
Kreutz, L.C., Ackermann, M.R., 1996. Porcine reproductive and respiratory syndrome virus enters cells through a low pH-dependent endocytic pathway. Virus Res. 42 (1–2), 137–147.
Laliberte, J.P., McGinnes, L.W., Peeples, M.E., Morrison, T.G., 2006. Integrity of membrane lipid rafts is necessary for the ordered assembly and release of infectious Newcastle disease virus particles. J. Virol. 80 (21), 10652–10662.
Li, G.M., Li, Y.G., Yamate, M., Li, S.M., Ikuta, K., 2007. Lipid rafts play an important role in the early stage of severe acute respiratory syndrome-coronavirus life cycle. Microbes Infect. 9 (1), 96–102.
Lingwood, D., Simons, K., 2010. Lipid rafts as a membrane-organizing principle. Science 327 (5961), 46–50.
Livak, K.J., Schmittgen, T.D., 2001. Analysis of relative gene expression data using real-time quantitative PCR and the 2(-Delta Delta C(T)) Method. Methods 25 (4), 402–408.
Meng, X.J., Paul, P.S., Halbur, P.G., 1994. Molecular cloning and nucleotide sequencing of the 3′-terminal genomic RNA of the porcine reproductive and respiratory syndrome virus. J. Gen. Virol. 75 (Pt 7), 1795–1801.
Mercer, J., Schelhaas, M., Helenius, A., 2010. Virus entry by endocytosis. Annu. Rev. Biochem. 79, 803–833.
Meulenberg, J.J., de Meijer, E.J., Moormann, R.J., 1993. Subgenomic RNAs of Lelystad virus contain a conserved leader-body junction sequence. J. Gen. Virol. 74 (Pt 8), 1697–1701.
Meulenberg, J.J., Petersen-den Besten, A., De Kluyver, E.P., Moormann, R.J., Schaaper, W.M., Wensvoort, G., 1995. Characterization of proteins encoded by ORFs 2 to 7 of Lelystad virus. Virology 206 (1), 155–163.
Munro, S., 2003. Lipid rafts: elusive or illusive? Cell 115 (4), 377–388.
Nauwynck, H.J., Duan, X., Favoreel, H.W., Van Oostveldt, P., Pensaert, M.B., 1999. Entry of porcine reproductive and respiratory syndrome virus into porcine alveolar macrophages via receptor-mediated endocytosis. J. Gen. Virol. 80 (Pt 2), 297–305.
Netherton, C.L., Wileman, T., 2011. Virus factories, double membrane vesicles and viroplasm generated in animal cells. Curr. Opin. Virol. 1 (5), 381–387.
Nguyen, D.H., Hildreth, J.E., 2000. Evidence for budding of human immunodeficiency virus type 1 selectively from glycolipid-enriched membrane lipid rafts. J. Virol. 74 (7), 3264–3272.
Nomura, R., Kiyota, A., Suzaki, E., Kataoka, K., Ohe, Y., Miyamoto, K., Senda, T., Fujimoto, T., 2004. Human coronavirus 229E binds to CD13 in rafts and enters the cell through caveolae. J. Virol. 78 (16), 8701–8708.
Ono, A., Freed, E.O., 2001. Plasma membrane rafts play a critical role in HIV-1 assembly and release. Proc. Natl. Acad. Sci. USA 98 (24), 13925–13930.
Patel, D., Opriessnig, T., Stein, D.A., Halbur, P.G., Meng, X.J., Iversen, P.L., Zhang, Y.J., 2008. Peptide-conjugated morpholino oligomers inhibit porcine reproductive and respiratory syndrome virus replication. Antiviral Res. 77 (2), 95–107.
Popik, W., Alce, T.M., Au, W.C., 2002. Human immunodeficiency virus type 1 uses lipid raft-colocalized CD4 and chemokine receptors for productive entry into CD4(+) T cells. J. Virol. 76 (10), 4709–4722.
Restrepo-Hartwig, M.A., Ahlquist, P., 1996. Brome mosaic virus helicase- and polymerase-like proteins colocalize on the endoplasmic reticulum at sites of viral RNA synthesis. J. Virol. 70 (12), 8908–8916.
Risselada, H.J., Marrink, S.J., 2008. The molecular face of lipid rafts in model membranes. Proc. Natl. Acad. Sci. USA 105 (45), 17367–17372.
Roberts, P.C., Compans, R.W., 1998. Host cell dependence of viral morphology. Proc. Natl. Acad. Sci. USA 95 (10), 5746–5751.
Rojek, J.M., Sanchez, A.B., Nguyen, N.T., de la Torre, J.C., Kunz, S., 2008. Different mechanisms of cell entry by human-pathogenic Old World and New World arenaviruses. J. Virol. 82 (15), 7677–7687.
Shi, S.T., Schiller, J.J., Kanjanahaluethai, A., Baker, S.C., Oh, J.W., Lai, M.M., 1999. Colocalization and membrane association of murine hepatitis virus gene 1 products and De novo-synthesized viral RNA in infected cells. J. Virol. 73 (7), 5957–5969.
Simons, K., Ikonen, E., 1997. Functional rafts in cell membranes. Nature 387 (6633), 569–572.
Simons, K., Toomre, D., 2000. Lipid rafts and signal transduction. Nat. Rev. Mol. Cell Biol. 1 (1), 31–39.
Simpson-Holley, M., Ellis, D., Fisher, D., Elton, D., McCauley, J., Digard, P., 2002. A functional link between the actin cytoskeleton and lipid rafts during budding of filamentous influenza virions. Virology 301 (2), 212–225.
Snijder, E.J., Meulenberg, J.J., 1998. The molecular biology of arteriviruses. J. Gen. Virol. 79 (Pt 5), 961–979.
Spilman, M.S., Welbon, C., Nelson, E., Dokland, T., 2009. Cryo-electron tomography of porcine reproductive and respiratory syndrome virus: organization of the nucleocapsid. J. Gen. Virol. 90 (Pt 3), 527–535.
Sun, Y., Xiao, S., Wang, D., Luo, R., Li, B., Chen, H., Fang, L., 2011. Cellular membrane cholesterol is required for porcine reproductive and respiratory syndrome virus entry and release in MARC-145 cells. Sci. China Life Sci. 54 (11), 1011–1018.
Thorp, E.B., Gallagher, T.M., 2004. Requirements for CEACAMs and cholesterol during murine coronavirus cell entry. J. Virol. 78 (6), 2682–2692.
Van Breedam, W., Delputte, P.L., Van Gorp, H., Misinzo, G., Vanderheijden, N., Duan, X., Nauwynck, H.J., 2010a. Porcine reproductive and respiratory syndrome virus entry into the porcine macrophage. J. Gen. Virol. 91 (Pt 7), 1659–1667.
Van Breedam, W., Van Gorp, H., Zhang, J.Q., Crocker, P.R., Delputte, P.L., Nauwynck, H.J., 2010b. The M/GP(5) glycoprotein complex of porcine reproductive and respiratory syndrome virus binds the sialoadhesin receptor in a sialic acid-dependent manner. PLoS Pathog. 6 (1), e1000730.
van der Meer, Y., Snijder, E.J., Dobbe, J.C., Schleich, S., Denison, M.R., Spaan, W.J., Locker, J.K., 1999. Localization of mouse hepatitis virus nonstructural proteins and RNA synthesis indicates a role for late endosomes in viral replication. J. Virol. 73 (9), 7641–7657.
Van Gorp, H., Van Breedam, W., Van Doorsselaere, J., Delputte, P.L., Nauwynck, H.J., 2010. Identification of the CD163 protein domains involved in infection of the porcine reproductive and respiratory syndrome virus. J. Virol. 84 (6), 3101–3105.
Wensvoort, G., Terpstra, C., Pol, J.M., ter Laak, E.A., Bloemraad, M., de Kluyver, E.P., Kragten, C., van Buiten, L., den Besten, A., Wagenaar, F., et al., 1991. Mystery swine disease in The Netherlands: the isolation of Lelystad virus. Vet. Q. 13 (3), 121–130.
Westaway, E.G., Mackenzie, J.M., Kenney, M.T., Jones, M.K., Khromykh, A.A., 1997. Ultrastructure of Kunjin virus-infected cells: colocalization of NS1 and NS3 with double-stranded RNA, and of NS2B with NS3, in virus-induced membrane structures. J. Virol. 71 (9), 6650–6661.
Yun, S.I., Lee, Y.M., 2013. Overview: replication of porcine reproductive and respiratory syndrome virus. J. Microbiol. 51 (6), 711–723.
Zhou, L., Yang, H., 2010. Porcine reproductive and respiratory syndrome in China. Virus Res. 154 (1–2), 31–37.
Ziebuhr, J., Snijder, E.J., Gorbalenya, A.E., 2000. Virus-encoded proteinases and proteolytic processing in the Nidovirales. J. Gen. Virol. 81 (Pt 4), 853–879.